Research Article | Vol. 27, No. 8 | 15 Apr 2019 | OPTICS EXPRESS 10814
Optics EXPRESS

Broadband dual-frequency comb spectroscopy in a rapid compression machine

ANTHONY D. DRAPER,[1,3] RYAN K. COLE,[1,3] AMANDA S. MAKOWIECKI,[1] JEFFREY MOHR,[2] ANDREW ZDANOWICZ,[2] ANTHONY MARCHESE,[2] NAZANIN HOGHOOGHI,[1] AND GREGORY B. RIEKER[1,*]

[1]*Precision Laser Diagnostics Laboratory, Department of Mechanical Engineering, University of Colorado Boulder, Boulder, CO 80309, USA*
[2]*Engines and Energy Conversion Laboratory, Department of Mechanical Engineering, Colorado State University, Fort Collins, CO 80523, USA*
[3]*Both authors contributed equally to this work.*
**greg.rieker@colorado.edu*

Abstract: We demonstrate fiber mode-locked dual-frequency comb spectroscopy for broadband, high-resolution measurements in a rapid compression machine (RCM). We apply an apodization technique to improve the short-term signal-to-noise-ratio (SNR), which enables broadband spectroscopy at combustion-relevant timescales. We measure the absorption on 24345 individual wavelength elements (comb teeth) between 5967 and 6133 cm^{-1} at 704 μs time resolution during a 12 ms compression of a CH_4-N_2 mixture. We discuss the effect of the apodization technique on the absorption spectra, and apply an identical effect to the spectral model during fitting to recover the mixture temperature. The fitted temperature is compared against an adiabatic model, and found to be in good agreement with expected trends. This work demonstrates the potential of DCS to be used as an *in situ* diagnostic tool for broadband, high-resolution measurements in engine-like environments.

1. Introduction

Infrared laser absorption spectroscopy is a useful technique for quantitative, nonintrusive measurement of gas temperature and species concentration in combustion systems [1]. Absorption spectroscopy measures the amount of light absorbed at specific wavelengths that correspond to rotational-vibrational transitions of the molecules in a gas mixture in order to determine the molecular populations in various quantum states. These populations can be linked back to temperature and species concentrations. The dynamic and harsh conditions found in many high-speed combustion systems place demanding requirements on laser absorption sensors. Specifically, the sensor must be able to quantify the absorption at high sensitivity and on short timescales. The ideal sensor would achieve these goals while also measuring over a broad frequency range at high resolution. Broad spectral bandwidth enables the measurement of multiple species that absorb at different frequencies, increases the temperature sensitivity and range by probing many rotational-vibrational energy levels, and allows the sensor to resolve absorption features over a large range of pressures and through spectral overlap of neighboring absorption transitions. This last capability is crucial as small molecules will exhibit narrow absorption features at ambient conditions which broaden and blend as the pressure increases.

In this paper, we demonstrate sub-millisecond-time-resolved, broadband dual-comb spectroscopy (DCS) with fiber mode-locked frequency combs at the high spectral resolution required to fully resolve absorption features across the full range of temperature and pressure conditions encountered in an engine-like environment. We recover temperature by fitting CH_4 absorption features spanning 166 cm^{-1} from 5967 to 6133 cm^{-1} at 0.0068 cm^{-1} tooth spacing, for a total of 24345 comb teeth. The absorption spectra are obtained at a time resolution of

#349766 https://doi.org/10.1364/OE.27.010814
Journal © 2019 Received 2 Nov 2018; revised 18 Jan 2019; accepted 28 Jan 2019; published 3 Apr 2019

Optics EXPRESS

704 μs in a rapid compression machine (RCM) operating from 1 to 21 bar and 294 to 566 K. The power-per-comb-mode is optimized and an apodization technique is used in Fourier processing to improve the short-term SNR. The apodization method introduces an instrument line shape, but this instrument line shape is known exactly, and can be unambiguously accounted for in the spectral fitting routine. This approach demonstrates the bandwidth and resolution benefits of mode-locked dual-comb spectroscopy at the timescales required for rapidly changing combustion environments.

1.1 Rapid compression machines

RCMs are typically used for laboratory studies of fuels and combustion kinetics, as well as sensor validation in realistic, engine-like conditions [2]. RCMs generally utilize one or more pneumatically driven pistons that, when released, rapidly compress a gas sample with a compression ratio of 10 to 20, resulting in elevated compressed pressures and temperatures (e.g. 10 to 30 bar, 500 to 1000 K). The compression process can occur in as little as 2 ms, and thus is often considered analogous to a single compression stroke of an internal combustion engine [2]. The combination of short timescales with rapidly varying thermodynamic conditions provides a realistic and demanding system in which sensors can be tested and validated.

The temperature evolution during the compression process is of particular interest for chemical kinetics studies due to its relation to reaction rate constants [1]. The temperature during the compression event T, can be approximated by Eq. (1) from a known initial temperature T_0, initial pressure P_0, the measured pressure during the compression $P(t)$, and the ratio of specific heats of the gas mixture γ [3].

$$\ln\left(\frac{P(t)}{P_0}\right) = \int_{T_0}^{T(t)} \frac{\gamma}{\gamma - 1}\frac{dT}{T} \tag{1}$$

This equation relies on the so-called adiabatic core assumption, namely that the compression occurs on such a short timescale that there is negligible heat transfer from the gas. This assumption will lose validity due to aerodynamic mixing during the compression as well as due to any chemical reactions that may occur [3,4]. After compression, the gas has additional time for heat transfer with the RCM walls, further deviating from the idealized process. Consequently, accurate temperature measurements are vital for combustion studies both in the time period of the compression process, as well as after the end of compression when the pistons are in their final position.

1.2 Laser absorption spectroscopy in engine-like environments

Many laser absorption sensors with narrow wavelength coverage have been demonstrated in rapid compression and shock tube environments with high sensitivity and time resolution [1,5]. Narrowband sensors observe a few select absorption features of a single species that have favorable temperature dependence within a range of interest. As the spectral bandwidth is small, pressure broadening effects can cause the absorption feature linewidth to exceed the measurement range. Together, these features create bounds on the species coverage and usable temperature and pressure ranges of the laser sensor.

Recently, a number of studies have published broadband absorption spectrometers to measure temperature within harsh environments such as an RCM [6–9]. Because broadband spectroscopy observes many absorption features, these techniques circumvent the limitations imposed by temperature sensitivity of particular features and pressure broadening that challenge narrowband sensors. The broadband nature additionally raises the possibility of multispecies monitoring. These sensors have relied upon external cavity diode lasers [8] or techniques such as Fourier domain mode locking [9] and supercontinuum generation [6,7] to record absorption spectra spanning hundreds of wavenumbers. Notably, Werblinski *et al.* demonstrate supercontinuum absorption spectroscopy in fired [6] and non-fired [7] RCMs.

Optics EXPRESS

The authors record spectra spanning more than 500 cm^{-1} at a rate of 10 kHz to measure time histories of temperature, pressure, and water vapor mole fraction in the compressed gas through a first derivative fitting approach. So far, broadband approaches in rapidly varying environments have limited spectral resolution (e.g. ~0.8–2.0 cm^{-1} [6–9]) that can limit the published results to pressures above 6 bar, below which the spectrometer resolution matches or exceeds the linewidth of the absorption features. In the context of RCMs, this limitation may not prove important. However, for diagnostics of reciprocating engines, where the characteristics of the combustion and exhaust strokes in a previous cycle might influence the initial conditions of the next cycle (and where models of the temperature evolution are very sensitive to the initial conditions before compression), having no limitations on the pressure range would be beneficial.

1.3 Dual frequency comb spectroscopy at short timescales

Frequency combs are laser sources that emit many discrete, evenly spaced frequencies of light, often referred to as comb teeth. DCS is an emerging technique that uses two frequency combs and is capable of simultaneous broad bandwidth and high resolution [10]. In DCS, a frequency comb is interfered with a second comb having slightly different tooth spacing in a massively parallel optical heterodyne approach. The heterodyne detection approach allows absorption to be resolved tooth-by-tooth, and for the data to be collected in the RF-domain with a single photodetector and no moving parts. In this configuration, the entire spectrum is recorded at a rate equal to the difference between the repetition rates of the two frequency combs, which is typically kHz or greater, as shown by past steady-state laboratory studies [11–14].

Currently, there are several classes of frequency comb that are capable of robust, portable operation: fiber mode-locked, modulator, and quantum cascade laser (QCL) combs. Mode-locked combs exhibit a train of short pulses comprising many thousands of comb teeth with optical frequency spacing matching the pulse repetition rate of the laser [15]. The intensity of the pulses lend themselves to nonlinear processes, and thus mode-locked combs are capable of nonlinear broadening to thousands of wavenumbers. Typically, the comb tooth spacing is very fine (0.003-0.03 cm^{-1}), as larger spacing requires high pulse repetition rate, which in turn would lead to short laser cavities and reduced peak power for nonlinear broadening.

Modulator combs are generated by electro-optic modulation of continuous-wave lasers [16,17]. The tooth spacing is given by the frequency of the RF source driving the modulators, thus the spacing can be tuned from 10^{-4} cm^{-1} to 1 cm^{-1}. However, the bandwidth of these combs is typically limited to a few wavenumbers and requires more complex approaches to achieve a broad bandwidth [18]. QCL frequency combs are semiconductor sources emitting in the mid-IR and THz [19]. They have modest bandwidth (40-100 cm^{-1}) in the mid-IR, with comparably large mode spacing (0.25-0.5 cm^{-1}), which leads to a relatively small number of comb teeth across the spectrum (a few hundred).

For a single dual-comb spectrum, the SNR in most cases is limited by the dynamic range of the detection system. In practice, the comb power striking the detector must be reduced to below the point where nonlinearities arise near detector saturation. Thus optimizing the power-per-comb-tooth striking the detector achieves the best noise characteristics. Comb systems operating with a small number of modes over a limited range, such as QCL and most modulator combs, are therefore capable of high short-term SNR at the expense of resolution and/or bandwidth [19]. Mode-locked combs with broad bandwidth and close tooth spacing place many more comb modes on the detector, spreading the power-per-mode and reducing short-term SNR, but with much higher bandwidth and resolution. At long timescales, the achievable SNR for DCS is driven by the ability to coherently average measured spectra. The ultimate SNR is therefore driven more by comb stability or the ability for software to correct for stability [14,20]. Consequently, absorption spectra for mode-locked DCS are typically averaged on the order of seconds to minutes to reach very high SNR. These constraints have

Optics EXPRESS

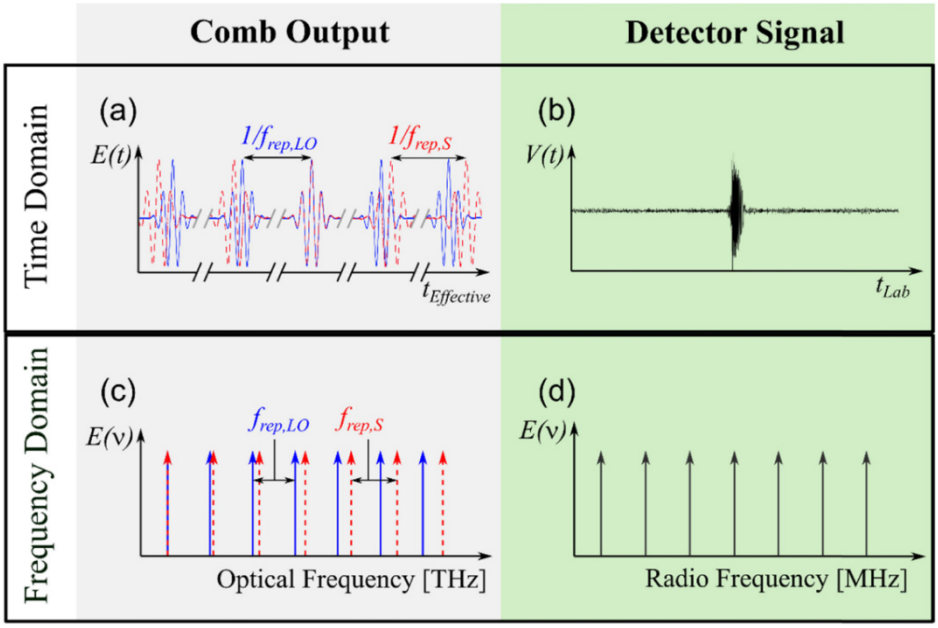

Fig. 1. Diagram showing the time and frequency domain representation of dual frequency comb spectroscopy. (a) Effective time domain schematic of femtosecond comb pulses originating from combs with different repetition rates, where the pulses of one comb "step through" the pulses of the other comb. The signal comb is shown in dashed red and the local oscillator comb in blue. (b) The time domain signal as recorded by the photodetector is a cross-correlation of the comb pulses – an interferogram – formed in laboratory time and with a "centerburst" when the pulses of the two combs are overlapping. (c) The comb teeth of the two combs represented in the optical frequency domain. The two comb repetition rates are fixed such that a unique heterodyne beat in the RF-domain is formed from pairs of comb teeth. (d) Individual comb teeth are resolved in the RF-domain by taking the Fourier Transform of the interferogram shown in (b).

generally positioned femtosecond mode-locked comb sources for broadband multispecies measurements in applications with relaxed time resolution.

A representative diagram of mode-locked DCS is shown in Fig. 1. DCS with mode-locked lasers is most easily described in the frequency domain, where each comb spectrum consists of evenly spaced frequency modes (teeth). Two frequency combs are phase locked to a stable reference such that the signal comb has repetition rate $f_{rep,S}$ and the second, local oscillator, comb has repetition rate $f_{rep,LO}$, where $f_{rep,S} - f_{rep,LO} = \Delta f_{rep}$. Moving across the spectrum, the optical frequency of each pair of fast and slow comb teeth differ by a frequency $n\Delta f_{rep}$, where n is an integer number of tooth pairs from the point where the frequencies of a pair of teeth exactly overlap. This difference frequency is detected on a photodiode as a heterodyne beat frequency, effectively mapping the magnitude of each pair of comb teeth from the optical domain into the RF-domain as shown in Fig. 1(d).

DCS can be described equivalently in the time domain as two femtosecond pulse trains with different repetition rates. In the frame of a pulse emitted by the signal comb, pulses from the local oscillator comb iteratively step through the signal comb pulse at an effective time step of $\Delta T_E = \Delta f_{rep} / (f_{rep,S} f_{rep,LO})$ [10]. These pulse trains are incident on a photodetector, such that they form a cross-correlation between the electric fields of the different comb pulses (termed an interferogram), that can be seen in Fig. 1(b), which exhibits an intense centerburst when the pulses of the combs are overlapping in time. The interferogram is digitized by commercial electronics with a laboratory time step between data points of $\Delta T_L = 1/f_{rep,LO}$.

Optics EXPRESS

Each interferogram is constructed of $N = f_{rep,LO} / \Delta f_{rep}$ individual points, and thus the laboratory time to acquire a single interferogram is given by $t_{acq} = 1/\Delta f_{rep}$. The frequency domain spectrum described in the preceding paragraph is the Fourier transform of the time domain interferogram. A more detailed description of the DCS method applied here is given in [10,21].

As mentioned above, the short term SNR of this detection method is typically limited due to the low optical power-per-comb-mode. As such, previous practical deployments of mobile, mode-locked dual-comb spectrometers [22,23] typically average for 60-120 seconds to build to high SNR. In order to resolve transient combustion phenomena, this averaging time must be decreased by upwards of a factor of 10,000. The first step to increasing the short-term SNR is to optimize the incident power on the photodetector. The approach is to maximize the power-per-comb-tooth (and thus the SNR) on the detector by filtering all comb teeth outside of the spectral region of interest, and to optimize the optical power incident on the photodetector such that it is operated just below the power level where detector non-linearity becomes large.

The short-term SNR for mode-locked DCS can be further increased by applying an apodization technique to the measured interferograms in post-processing. Most of the signal of interest in DCS is collected during the centerburst of the interferogram: when the pulses from the two combs are overlapping in time on the detector. The rest of the interferogram is still important to collect in order to obtain the right number of points for a full, comb-tooth-resolved spectrum, and because one must wait for the pulses of the two combs to overlap again. Apodization multiplies a function with the interferogram in order to retain the signal around the centerburst while filtering out the noise on the rest of the interferogram, which would subsequently become noise in the frequency domain. However, the cost of this technique is the addition of an instrumental line shape in the resulting absorption spectrum [24]. Many different apodization functions exist, such as the boxcar, triangular or extended Norton-Beer functions [24]. In this work, we apodize the interferograms with a boxcar function to increase the short-term SNR. The boxcar function was chosen due to its simplicity and the fact that it offers the narrowest instrument line shape function (and thus the highest spectral resolution) [24]. A more involved examination of apodization functions for this application can be found in [25].

The instrument line shape resulting from a boxcar apodization function is described analytically as Eq. (2) where Δ_E is the HWHM of the boxcar function in effective time, and ν is the frequency.

$$f(\nu) = 2\Delta_E \mathrm{sinc}\left(2\pi\Delta_E \nu\right) \tag{2}$$

Thus, the instrument line shape is perfectly known, and can therefore be applied to the absorption model that is used to fit the data. Because the same instrument line shape is added to the model and the data, the choice of apodization function does not significantly impact the fit between measurement and model, but does affect the resolution of the measurement itself. In order to demonstrate the feasibility of introducing the line shape function to the fitting routine, a 1 bar and 300 K CO line near 6297.5 cm^{-1} was measured in a static configuration with the fiber mode-locked dual-comb spectrometer discussed in the following section. This data was coherently averaged over a period of 10 minutes to reach very high SNR so that the effect of the apodization process and match with the model is readily apparent. A boxcar apodization was applied to both the experimental data and the HITRAN 2016-based absorption model. Figure 2 shows the agreement between the apodized model and measurement. As the instrument line shape is a known analytical function, the model replicates the effects of apodization exactly. Therefore, the outcome of a fitting routine used to determine the temperature or species concentration is unbiased by the addition of the instrument line shape.

Optics EXPRESS

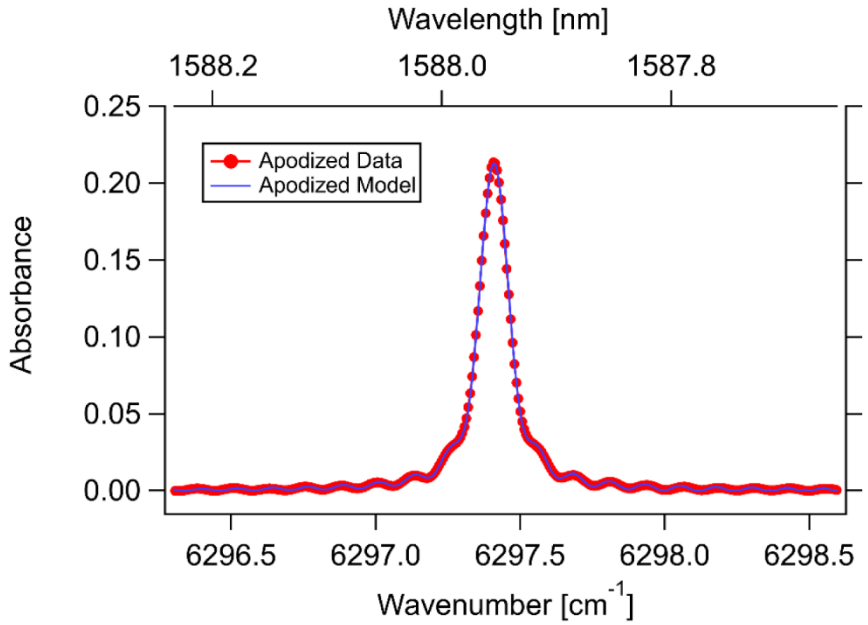

Fig. 2. Measured CO absorption feature near 6297.5 cm^{-1}, with the same apodization applied to the measured interferogram (red) and the model (blue). The instrument line shape from apodization is apparent, but is well captured by the model. This data was coherently averaged for a period of 10 minutes to increase the signal to noise ratio and emphasize the effect of the added instrument line shape.

2. Experimental setup

The RCM employed in this work was manufactured by Marine Technologies Ltd., and is housed in the Engines and Energy Conversion Laboratory at Colorado State University (CSU). The RCM employs dual piston design with creviced pistons that reduce the effects of aerodynamic mixing during the compression process [3,26], and was configured for a compression ratio of 12.5. Optical access to the combustion chamber is provided through two sapphire windows with a 3° wedge to discourage etalon interference effects. Gas pressure is measured before the compression process using an Omega DPG409 pressure transducer (accuracy 0.08% of reading), and monitored during the compression stroke using a Kistler 603B pressure sensor (accuracy 1% of reading). A detailed description of the CSU RCM facility can be found in [26,27].

The near-IR mobile dual-comb spectrometer used for this measurement has a nominal repetition rate of 204 MHz and is centered at 6452 cm^{-1} (1550 nm) with an optical bandwidth of approximately 1250 cm^{-1} (~300 nm). Both erbium fiber frequency combs are self-referenced, and the repetition rates are locked to a known cw laser, giving the system a precisely known and stable frequency axis. Further details for this spectrometer are given in [22-23,28]. The two frequency combs were phase locked with $\Delta f_{rep} = 2837\,Hz$, giving a single spectrum acquisition time of 352 µs. The laser light from both combs was combined using a fiberized coupler and subsequently filtered to cover 5967-6133 cm^{-1}. The point spacing of the spectrum was set by the laser repetition rates to be 0.0068 cm^{-1}, which resulted in 24345 individually resolved comb teeth accessible for fitting. Light from the DCS was delivered with single mode fiber to the RCM, collimated, and passed though the 4.63 cm combustion chamber. Laser light leaving the RCM was incident on a DC-coupled fast photodetector (ThorLabs PDA10CF) where the two combs interfered to generate a

Optics EXPRESS

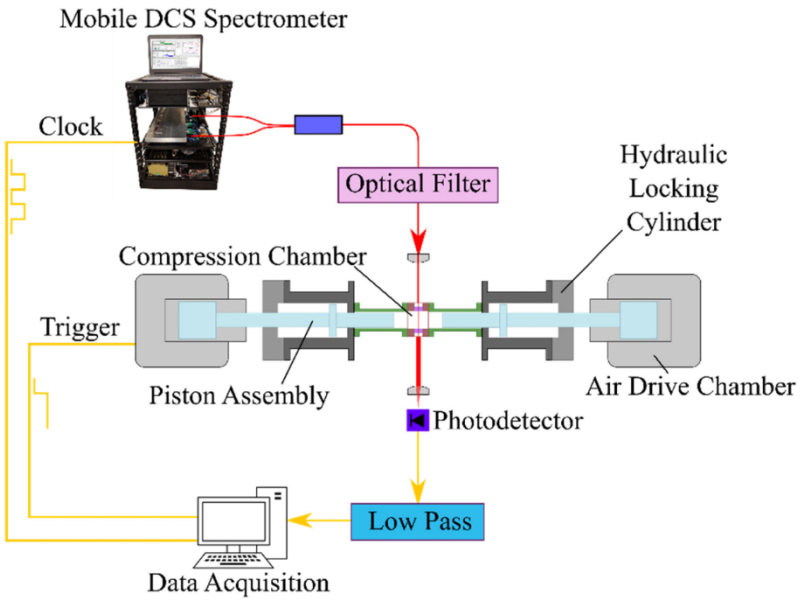

Fig. 3. Schematic of experimental setup. The mobile DCS supplies light via single-mode fiber to a collimator, which transmits the light through the RCM combustion chamber, and is then received through a convex focusing lens onto a fast photodetector. The resulting signal is low-pass filtered before being collected with the data acquisition system. The spectrometer also provides a clock signal to the data acquisition, and the RCM start switch is linked to enable synchronous collection.

heterodyne beat structure. The detector output was low-pass filtered (100 MHz bandwidth), and recorded with a 250 MS/s digitizer. A schematic of this experimental configuration is shown in Fig. 3.

The RCM combustion chamber was maintained at 294 ± 0.5 K, the pistons retracted and locked, and the chamber evacuated to 6.9 ± 0.8 mbar. A vacuum data set was collected to aid in baseline correction in post-processing before compression. Subsequently, CH_4 was first added to the chamber, and then N_2, to give an initial pressure of 1001 mbar, with a CH_4 mole fraction of 0.750. Data collection was triggered synchronous to the RCM pistons being released via a common start signal. Time-domain interferograms were collected during the compression process through an automated LabVIEW program.

3. Results and analysis

3.1 Data processing

Every two interferograms measured through the RCM were averaged for an overall measurement time resolution of 704 µs. A boxcar apodization HWHM of $\Delta_E = 229\,ps$ was applied to each binned interferogram, yielding a FWHM of the instrument line shape of 0.088 cm^{-1}. The spectral resolution with the instrument line shape can be estimated from Rayleigh's definition as $1/\Delta_E = 0.15\,cm^{-1}$, which yields the experimental spectral resolution [24,29]. This degree of apodization was selected in order to maintain the ability to resolve the CH_4 absorption features at 1 bar and 298 K before the RCM compression process.

Optics EXPRESS

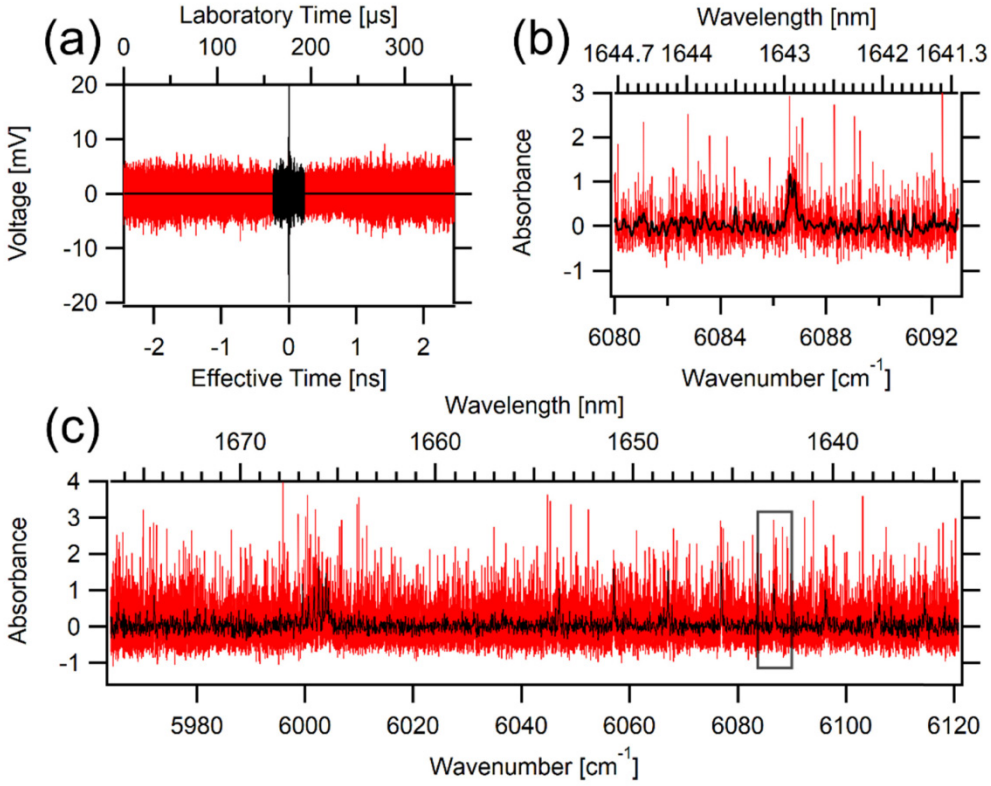

Fig. 4. Measured absorbance spectra at 1 bar and 294 K with 704 μs time resolution just prior to the compression. The red traces are the unapodized data and the black traces are apodized. (a) Interferogram with both the laboratory and effective timescales shown, (b) Zoomed CH_4 absorption feature for the region indicated on panel c, and (c) Full measured spectrum.

Apodized interferograms were subsequently Fourier transformed to yield the CH_4 transmission spectrum through the RCM. Each transmission spectrum was baseline corrected using the vacuum background data set and converted to absorbance units with Beer's law. A polynomial baseline fitting routine (described in [30]) was used to correct residual baseline irregularities caused by subtle differences between the vacuum background and compression data sets. Experimental spectra at the initial conditions are shown in Fig. 4 to illustrate theeffect of apodization. The resulting SNR benefit is dramatically evident, and results in roughly a factor of 7 improvement over the non-apodized spectrum. From the zoom view shown in Fig. 4(b), one can see the emergence of the CH_4 absorption feature from the noise using the apodization approach.

3.2 Temperature fitting

A Levenberg-Marquardt algorithm was utilized to fit a model generated from the HITRAN 2016 database [31] with the Python HAPI package [32] to each baseline corrected spectrum. The mixture mole fraction and pressure were held constant and temperature was allowed to vary (with an initial guess from GASEQ calculations, described later). The resulting temperature fit is shown in Fig. 5.

Optics EXPRESS

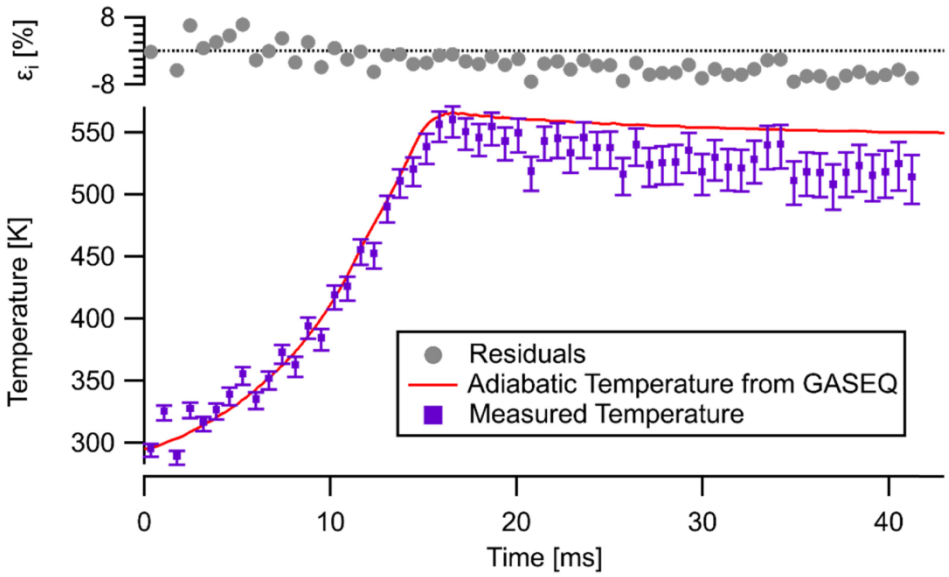

Fig. 5. DCS-measured temperature from broadband fitting of the apodized spectra (purple). The red trace is the adiabatic temperature calculated using GASEQ, while the gray represents the residual percent error.

Using the measured pressure, the compression temperature was calculated with GASEQ, a thermodynamic equilibrium software [33]. The measured temperature tracks well with the calculation during the compression process, 0 to 15 ms, and reaches a peak temperature 6 K lower than the 566 K predicted by GASEQ. This agreement is likely within the uncertainty of the GASEQ calculation, which we do not directly estimate here, but is affected by uncertainty in the initial temperature, gas composition, and measured pressure. The dual-comb measured temperature decreases faster than the calculation once the pistons lock at the end of compression, ultimately reading approximately 19 K lower than the GASEQ predicted temperature after 25 ms. This deviation could arise from several effects. For example, the formation of cold boundary layers can influence the path-averaged temperature measurement to a value that is slightly lower than the GASEQ calculated temperature [3,5]. In addition, the effect of the thermal boundary layers could be enhanced through aerodynamic mixing of the gas in the compressed volume, which is not fully eliminated by the creviced piston design [3]. Additional mixing effects may also arise due to the slight asymmetry in the timing of the two opposing pistons. With further investigations using a broadband spectrometer, it could be possible to determine the temperature distribution along the line of sight by measuring multiple lines with varying lower state energies [34].

The systematic uncertainty of the frequency comb measurement is represented by the uncertainty bars on Fig. 5. The uncertainties of the pressure transducers, the physical tolerance stack-up of the path length, and the initial temperature were included as input values into the fitting routine to determine their influence on the measured temperature values. At the initial onset of the compression, the uncertainty is ± 6 K, which increases to ± 20 K at the end of data collection. The increase is a result of increasing pressure transducer uncertainty and the greater influence of the uncertainty in the initial conditions as one scales to higher compression.

The precision of the measurement was assessed using the residual between the measured and calculated values. The residual percent error was split into two sets: values leading up to and including the peak compression, and values from the peak until the end of the data set. The linear trends were removed from the residuals, the normality of the two sets verified through the Shapiro-Wilk test, and their standard deviations calculated. Up until the

Optics EXPRESS

compression peak, the standard deviation of the residual percent error is ± 3.1%, and ± 1.5% afterwards. In the relatively constant temperatures following the compression peak, the 1.5% residual corresponds to approximately ± 8.5 K measurement precision.

It is interesting to note that while the absorbance noise of this measurement is significantly higher than that of a typical diode laser or WMS scan, the fit to the data results in a temperature measurement with single-digit Kelvin precision. The high precision and low uncertainty despite the absorbance noise is due to the broadband nature of the comb – the fit includes a very large number of comb teeth (24345) probing a large number of CH_4 absorption features. Each spectral fit is constrained across the tens of thousands of comb teeth, which improves precision. Across the measured bandwidth, the HITRAN database predicts 2430 individual methane absorption lines which contribute to approximately 19 distinguishable features in the measured spectrum [31]. Each feature has a unique scaling of its magnitude with temperature, further improving accuracy and temperature sensitivity. These effects lead to a precise and robust fit between the model and the measured spectrum.

4. Conclusions

We demonstrate high-speed, broadband, mode-locked dual frequency comb spectroscopy in an RCM by measuring the temperature of a CH_4-N_2 gas mixture with 704 μs time resolution. Absorption features were measured with 24345 comb teeth between 5967 and 6133 cm^{-1}. The short-term SNR of the portable spectrometer was improved through optical power optimization and the application of a boxcar apodization function to the interferograms in post-processing. The apodization technique introduced an exactly known instrument line shape, with a theoretical spectral resolution of 0.15 cm^{-1}. With this resolution, absorption features are fully resolved throughout the full range of temperatures and pressures encountered in the compression. The compressed gas temperature was measured using a broadband fitting algorithm with a model that incorporated the exact instrument line shape introduced from apodization. The fitted temperatures agree well with the predicted adiabatic values calculated from the measured pressure. This comparison shows a 6 K under prediction of the 566 K peak as well as indications of the breakdown of the adiabatic assumption after the end of compression. These results indicate that mode-locked DCS can serve as a powerful diagnostic tool for broadband, high resolution spectroscopy in transient combustion environments.

The techniques presented in this paper will see enhanced applicability when combined with rapidly evolving mid-IR mode-locked dual-comb technology [11–13,35,36]. These spectrometers will leverage the bandwidth and fine mode spacing of existing DCS systems with higher sensitivity afforded by the stronger absorption cross sections characteristic of the mid-infrared. The increase in sensitivity will enable temperature measurements at higher time resolution, while the high bandwidth will enable multiple combustion-relevant species to be measured with a single spectrometer.

Funding

Air Force Office of Scientific Research Grant (FA9550-17-1-0224), NASA Fellowship (18-PLANET18R-0018), Defense Advanced Projects Agency (W31P4Q-15-1-0011), and the National Science Foundation (CBET 1454496).

Acknowledgments

We would like to thank Dr. Colin Gould and Dr. Azer Yalin for their help preparing for the RCM experiment. The views and conclusions contained in this document are those of the authors and should not be interpreted as representing the official policies, either expressed or implied, of the Defense Advanced Research Projects Agency, the U.S. Army, or the U.S. Government.

Optics EXPRESS

References

1. C. S. Goldenstein, R. M. Spearrin, J. B. Jeffries, and R. K. Hanson, "Infrared laser-absorption sensing for combustion gases," Pror. Energy Combust. Sci. **60**, 132–176 (2017).
2. S. S. Goldsborough, S. Hochgreb, G. Vanhove, M. S. Wooldridge, H. J. Curran, and C.-J. Sung, "Advances in rapid compression machine studies of low- and intermediate-temperature autoignition phenomena," Pror. Energy Combust. Sci. **63**(Supplement C), 1–78 (2017).
3. G. Mittal and C.-J. Sung, "Aerodynamics inside a rapid compression machine," Combust. Flame **145**(1), 160–180 (2006).
4. B. W. Weber, C.-J. Sung, and M. W. Renfro, "On the uncertainty of temperature estimation in a rapid compression machine," Combust. Flame **162**(6), 2518–2528 (2015).
5. E. F. Nasir and A. Farooq, "Time-resolved temperature measurements in a rapid compression machine using quantum cascade laser absorption in the intrapulse mode," Proc. Combust. Inst. **36**(3), 4453–4460 (2017).
6. T. Werblinski, P. Fendt, L. Zigan, and S. Will, "High-speed combustion diagnostics in a rapid compression machine by broadband supercontinuum absorption spectroscopy," Appl. Opt. **56**(15), 4443–4453 (2017).
7. T. Werblinski, S. Kleindienst, R. Engelbrecht, L. Zigan, and S. Will, "Supercontinuum based absorption spectrometer for cycle-resolved multiparameter measurements in a rapid compression machine," Appl. Opt. **55**(17), 4564–4574 (2016).
8. C. L. Hagen and S. T. Sanders, "Investigation of multi-species (H 2 O 2 and H 2 O) sensing and thermometry in an HCCI engine by wavelength-agile absorption spectroscopy," Meas. Sci. Technol. **18**(7), 1992–1998 (2007).
9. L. A. Kranendonk, J. W. Walewski, T. Kim, and S. T. Sanders, "Wavelength-agile sensor applied for HCCI engine measurements," Proc. Combust. Inst. **30**(1), 1619–1627 (2005).
10. I. Coddington, N. Newbury, and W. Swann, "Dual-comb spectroscopy," Optica **3**(4), 414 (2016).
11. F. C. Cruz, D. L. Maser, T. Johnson, G. Ycas, A. Klose, F. R. Giorgetta, I. Coddington, and S. A. Diddams, "Mid-infrared optical frequency combs based on difference frequency generation for molecular spectroscopy," Opt. Express **23**(20), 26814–26824 (2015).
12. F. Keilmann, C. Gohle, and R. Holzwarth, "Time-domain mid-infrared frequency-comb spectrometer," Opt. Lett. **29**(13), 1542–1544 (2004).
13. A. Schliesser, M. Brehm, F. Keilmann, and D. van der Weide, "Frequency-comb infrared spectrometer for rapid, remote chemical sensing," Opt. Express **13**(22), 9029–9038 (2005).
14. T. Ideguchi, A. Poisson, G. Guelachvili, N. Picqué, and T. W. Hänsch, "Adaptive real-time dual-comb spectroscopy," Nat. Commun. **5**(1), 3375 (2014).
15. J. L. Hall, "Nobel Lecture: Defining and measuring optical frequencies," Rev. Mod. Phys. **78**(4), 1279–1295 (2006).
16. T. Kobayashi, T. Sueta, Y. Cho, and Y. Matsuo, "High□repetition□rate optical pulse generator using a Fabry□Perot electro□optic modulator," Appl. Phys. Lett. **21**(8), 341–343 (1972).
17. D. A. Long, A. J. Fleisher, K. O. Douglass, S. E. Maxwell, K. Bielska, J. T. Hodges, and D. F. Plusquellic, "Multiheterodyne spectroscopy with optical frequency combs generated from a continuous-wave laser," Opt. Lett. **39**(9), 2688–2690 (2014).
18. D. R. Carlson, D. D. Hickstein, W. Zhang, A. J. Metcalf, F. Quinlan, S. A. Diddams, and S. B. Papp, "Ultrafast electro-optic light with subcycle control," Science **361**(6409), 1358–1363 (2018).
19. G. Villares, A. Hugi, S. Blaser, and J. Faist, "Dual-comb spectroscopy based on quantum-cascade-laser frequency combs," Nat. Commun. **5**(1), 5192 (2014).
20. J. Roy, J.-D. Deschênes, S. Potvin, and J. Genest, "Continuous real-time correction and averaging for frequency comb interferometry," Opt. Express **20**(20), 21932–21939 (2012).
21. I. Coddington, W. C. Swann, and N. R. Newbury, "Coherent dual-comb spectroscopy at high signal-to-noise ratio," Phys. Rev. A **82**(4), 043817 (2010).
22. S. Coburn, C. B. Alden, R. Wright, K. Cossel, E. Baumann, G.-W. Truong, F. Giorgetta, C. Sweeney, N. R. Newbury, K. Prasad, I. Coddington, and G. B. Rieker, "Regional trace-gas source attribution using a field-deployed dual frequency comb spectrometer," Optica **5**(4), 320–327 (2018).
23. P. J. Schroeder, R. J. Wright, S. Coburn, B. Sodergren, K. C. Cossel, S. Droste, G. W. Truong, E. Baumann, F. R. Giorgetta, I. Coddington, N. R. Newbury, and G. B. Rieker, "Dual frequency comb laser absorption spectroscopy in a 16 MW gas turbine exhaust," Proc. Combust. Inst. **36**(3), 4565–4573 (2017).
24. P. R. Griffiths and J. A. D. Haseth, *Fourier Transform Infrared Spectrometry* (John Wiley & Sons, 2007).
25. A. D. Torres, R. K. Cole, J. Mohr, A. Zdanawicz, C. Gould, A. Marchese, and G. Rieker, "Progress Toward Dual Frequency Comb Spectroscopy in a Rapid Compression Machine," in *AIAA Scitech 2019 Forum* (American Institute of Aeronautics and Astronautics, 2019).
26. A. Boissiere, "Effect of additives on laser ignition and compression ignition of methane and hydrocarbons in a rapid compression machine," ProQuest Dissertations Publishing (2016).
27. C. Dumitrache, M. Baumgardner, A. Boissiere, A. Maria, J. Roucis, A. J. Marchese, and A. Yalin, "A study of laser induced ignition of methane–air mixtures inside a Rapid Compression Machine," Proc. Combust. Inst. **36**(3), 3431–3439 (2017).
28. G.-W. Truong, E. M. Waxman, K. C. Cossel, E. Baumann, A. Klose, F. R. Giorgetta, W. C. Swann, N. R. Newbury, and I. Coddington, "Accurate frequency referencing for fieldable dual-comb spectroscopy," Opt. Express **24**(26), 30495–30504 (2016).

Optics EXPRESS

29. N. R. Newbury, I. Coddington, and W. Swann, "Sensitivity of coherent dual-comb spectroscopy," Opt. Express **18**(8), 7929–7945 (2010).
30. P. J. Schroeder, D. J. Pfotenhauer, J. Yang, F. R. Giorgetta, W. C. Swann, I. Coddington, N. R. Newbury, and G. B. Rieker, "High temperature comparison of the HITRAN2012 and HITEMP2010 water vapor absorption databases to frequency comb measurements," J. Quant. Spectrosc. Radiat. Transf. **203**, 194–205 (2017).
31. I. E. Gordon, L. S. Rothman, C. Hill, R. V. Kochanov, Y. Tan, P. F. Bernath, M. Birk, V. Boudon, A. Campargue, K. V. Chance, B. J. Drouin, J.-M. Flaud, R. R. Gamache, J. T. Hodges, D. Jacquemart, V. I. Perevalov, A. Perrin, K. P. Shine, M.-A. H. Smith, J. Tennyson, G. C. Toon, H. Tran, V. G. Tyuterev, A. Barbe, A. G. Császár, V. M. Devi, T. Furtenbacher, J. J. Harrison, J.-M. Hartmann, A. Jolly, T. J. Johnson, T. Karman, I. Kleiner, A. A. Kyuberis, J. Loos, O. M. Lyulin, S. T. Massie, S. N. Mikhailenko, N. Moazzen-Ahmadi, H. S. P. Müller, O. V. Naumenko, A. V. Nikitin, O. L. Polyansky, M. Rey, M. Rotger, S. W. Sharpe, K. Sung, E. Starikova, S. A. Tashkun, J. V. Auwera, G. Wagner, J. Wilzewski, P. Wcisło, S. Yu, and E. J. Zak, "The HITRAN2016 molecular spectroscopic database," J. Quant. Spectrosc. Radiat. Transf. **203**, 3–69 (2017).
32. R. V. Kochanov, I. E. Gordon, L. S. Rothman, P. Wcisło, C. Hill, and J. S. Wilzewski, "HITRAN Application Programming Interface (HAPI): A comprehensive approach to working with spectroscopic data," J. Quant. Spectrosc. Radiat. Transf. **177**, 15–30 (2016).
33. C. Morley, *GASEQ* (2005).
34. S. T. Sanders, J. Wang, J. B. Jeffries, and R. K. Hanson, "Diode-laser absorption sensor for line-of-sight gas temperature distributions," Appl. Opt. **40**(24), 4404–4415 (2001).
35. E. Baumann, F. R. Giorgetta, W. C. Swann, A. M. Zolot, I. Coddington, and N. R. Newbury, "Spectroscopy of the methane ν 3 band with an accurate midinfrared coherent dual-comb spectrometer," Phys. Rev. A **84**(6), 062513 (2011).
36. O. Kara, L. Maidment, T. Gardiner, P. G. Schunemann, and D. T. Reid, "Dual-comb spectroscopy in the spectral fingerprint region using OPGaP optical parametric oscillators," Opt. Express **25**(26), 32713–32721 (2017).